

Design of a Decentralized PID Controller Using the Relative Gain Array Technique for a Coupled Flotation Process

N. Tshemesese-Mvandaba* and M. E. S. Mnguni

Department of Electrical, Electronics and Computer Engineering, Cape Peninsula University of Technology, South Africa

Email: tshemesen@cput.ac.za (N.T.M.), mngunim@cput.ac.za (M.E.S.M.)

Abstract—This study focuses on the design of the decentralized Proportional-Integral-Derivative (PID) controller for a coupled flotation system. It emphasizes the difficulties encountered when dealing with interconnected Multiple-Input Multiple-Output (MIMO) systems that cannot be effectively regulated using traditional linear feedback controllers. The significance of this article lies in its examination of how the Relative Gain Array (RGA) can be utilized to mitigate the impact of process connections. With the use of a thoughtful selection of single-loop pairings, the decentralized controller is created following the RGA technique. The decentralized controller that has been developed serves the purpose of reducing the influence caused by process interfaces. A set-point tracking technique, based on Internal Model Controllers (IMCs) is adopted in the design. The system time response and overshoot were also analyzed. The paper proposed a decentralized control mechanism and provided a comprehensive process for applying it to both the system under investigation and different MIMO industrial processes. The performance of the suggested closed-loop system was simulated and confirmed using Matlab/Simulink.

Index Terms—Flotation process, Multiple Inputs Multiple Outputs (MIMO) systems, Proportional-Integral-Derivative (PID), relative gain array, internal model controller

I. INTRODUCTION

Proportional-Integral (PI) and Proportional-Integral-Derivative (PID) controllers are the most frequently utilized controllers across numerous industries [1, 2]. They provide functionalities that allow systems to handle transient and steady-state responses. Aside from their simplicity in construction, proportional-integral-derivative controllers possess the capability to provide valuable solutions to a variety of practical challenges, as indicated in [3, 4]. The PID control variant uses multiple methods to calculate integral and derivative values. Furthermore, a self-adjusting PID controller using Adaptive Neuro-Fuzzy (ANF) technology was presented in [4] for the nuclear core reactor application. This article utilizes the adaptive controller approach to enhance the performance characteristics of the Pressurized Water Reactor (PWR). According to [5], Model Predictive

Control (MPC) is one of the most effective advanced controllers for improving flotation performance. However, if the perspective prediction is not formulated correctly, control performance will be poor even if the model is correct. This control method depends on a data model that represents numerous model coefficients used to portray the dynamics of the process. Over the past few years, control researchers have developed an interest in exploring trajectory-tracking control methodologies, for many reasons as exemplified by the work presented in [6]. Vu *et al.* [6] introduced innovative methods to guarantee the Uniformly Ultimately Bounded (UUB) stability of the enclosed dynamic system.

The difficulties encountered when dealing with flotation systems or any Multiple-Input Multiple-Output (MIMO) process that cannot be effectively regulated using traditional linear feedback controllers, as emphasized in [2, 7–9], serve as the motivational factors for this paper. Euzebio *et al.* [1] indicated that the MIMO control issues are frequently solved with decentralized PID control systems. However, decentralized controllers are unable to eliminate plant interactions in multi-variable systems, hence Euzebio *et al.* [1] dealt with these interactions at the controller tuning stage. This paper adopted a Relative Gain Array (RGA) to mitigate the impact of process interactions. The study of MIMO or multi-variable systems from a research perspective represents a novel scientific approach that examines how the interactions and connections among components contribute to the overall behaviors of a MIMO system. These interactions also form the system's relationship with its surroundings, as discussed in [2] and [10]. Due to interactions between processes and loops, designing a controller for flotation systems is complicated, and creates a demanding task for the control.

As outlined in various articles, there exist two primary categories of MIMO controller design approaches: centralized and decentralized controllers. The literature, as in [10, 11], has presented numerous techniques for creating centralized controllers. Many effective algorithms, such as the Differential Search Algorithm (DSA), a Real Coded Genetic Algorithm Through Simulated Binary Crossover (RGA-SBX), Chaotic Gravitational Search Algorithm (CGSA), and Particle Swarm Optimization (PSO) were examined in [3] in comparison to the best cross-coupled nonlinear PID

Manuscript received June 14, 2023; revised September 7, 2023; accepted October 12, 2023; published February 2, 2024.

*Corresponding author

controller design. The results indicate that PID controllers exhibit superior performance compared to alternative control methods in multi-variable systems. Hence, it is still recommended to use them. The recent review demonstrated a notable research contribution [6], this research has produced an algorithm that can facilitate tracking within cascade control design. This was achieved through the application of Adaptive Reinforcement Learning (ARL).

The flotation column system is one of the multi-variable processes with an objective of metallurgical performance control to ensure compliance with the process operation as shown by the grade and recovery of valuable minerals [10, 12–17]. An essential industrial procedure for extracting rich minerals from gangue minerals is froth flotation [17]. Zhang and Xu [16] indicated that it is not enough to rely solely on the employees' observation of the froth due to the complicated nature of the flotation process. Furthermore, the froth is a significant source of data regarding the flotation system's working status, hence control and monitoring of its state of operation is essential. Based on the findings from the investigation conducted in [18], it is encouraging to note that the modified variables are well-industrial instrumented and dependable in a regulatory control layer at an industrial flotation facility. However, further examinations are required to fine-tune the substance response variable for effective management of the plant's metallurgical performance [18].

Many advancements in controller design methods have been made focusing on improving control of the multi-variable processes. As highlighted in [19, 20], the flotation process came across a wide array of challenges that necessitate the application of intelligent control techniques. Various elements influencing the flotation process were reviewed and presented in [21] with particular emphasis on Phosphate Ores. However, the operational adaptability inherent in the decentralized approach substantially enhances the industrial applicability of PI and PID schemes [17]. The interconnections that exist between the control and manipulated loops are the major challenge in decentralizing the system model for MIMO systems. The popularity of decentralized control is due to its simplicity and option availabilities of loop-independent operation [22, 23]. Historically, PID control methods have been predominant in industrial applications [24]. However, it might be challenging to identify the suitable PID control ideal tuning parameters, particularly for processes with multiple variables as indicated in [8].

When it comes to controlling interconnected systems, three major challenges arise. One is the practical limitation of the number and configuration of feedback loops, which supports decentralized control structures. The presence of hesitations in both subsystems and interconnections adds additional concern. Another concern is the control systems' consistency in the event of component failures. The likelihood of experiencing malfunctions in practical engineering systems is significant, and these issues have the potential to induce instabilities in the system's functioning [25].

The RGA approach is used to determine suitable input-

output pairing while developing decentralized diagonal controllers. According to [1] and [26], RGA was introduced as a measure of process interactions in multi-input, multi-output control problems [27]. Due to its simplicity and utility, the RGA analysis has been widely used to identify capable decentralized multi-loop control systems based on limited information, and steady-state gains. It is noted that [28] derived the controller settings for linear and non-linear models from the Internal Model Controller (IMC) and Tantu & Lieslehto (TL) tuning relations, these parameters showed proper setpoint tracking and disturbance rejections. However, in some cases, there are high chances of encountering failures in real engineering systems, and they could cause instabilities in the system's operation [25]. Since the decentralized system involves interaction, it can be estimated by the Relative Gain Analysis (RGA) index and Niederlinski method by pairing the manipulated and control variables for a stable system [2]. It is important to note that each element in the RGA matrix for a $n \times n$ system represents the ratio of the open-loop gain for a specific loop in the situation where all other loops are open, to the closed-loop gain for that loop when all other loops are closed [26–29].

The significance of this paper is based on the assessment of using RGA to mitigate the impacts of process connections. The approach applied in this study has played a role in identifying optimal combinations that result in efficient controller performance in the investigated MIMO system.

The structure of the paper is as follows: In Section II, the analysis of the model and the design of controllers are presented. This involves utilizing the PID algorithm for configuring control parameters, along with an internal model controller approach to manage process interactions. Section III outlines the assessment of the model and showcases the outcomes through various case studies. Findings are discussed in Section IV, and Section V provides the paper's conclusion.

II. MODEL ANALYSIS AND CONTROLLER DESIGN

Due to the complexity of the flotation system as a multi-variable process, determining suitable connections without testing is challenging. Therefore, RGA aids in categorizing appropriate loop connections [27, 30, 31]. In the context of multi-variable controller design, the RGA approach delivers two crucial types of information. Firstly, it offers a gauge of process interactions, and secondly, it provides a set of suggestions for the optimal pairing to mitigate the effects of these interactions. The procedure and the discussion of the loop pairing based on interaction analysis have been used in this paper.

Fig. 1 shows a block diagram illustrating the MIMO system. This diagram presents the use of two single-loop controllers as a simple method of controlling this MIMO system, where each controller is responsible for regulating one specific loop. To achieve this, one must first decide how the controllers should be connected, which means $h(s)$ in Fig. 1 should be controlled by U_1 , this is called the pairing problem. This challenge can be simple if there is little interaction between the loops,

which can be identified from the reactions of all outputs to all inputs.

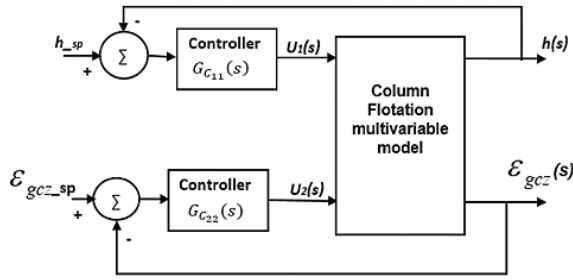


Fig. 1. Loop interactions for a 2×2 multi-variable system.

Next, we proceed with the analysis of interactions and the application of RGA technique.

Consider the mathematical model presented as

$$\mathbf{G}(s) = \begin{bmatrix} h(s) \\ \varepsilon_{gcz}(s) \end{bmatrix} = \begin{bmatrix} G_{11}(s) & G_{12}(s) \\ G_{21}(s) & G_{22}(s) \end{bmatrix} \quad (1)$$

where the transfer functions of $G_{11}(s)$, $G_{12}(s)$, $G_{21}(s)$, and $G_{22}(s)$ were given in [13].

The RGA is concerned with steady-state conditions. Now let \mathbf{K} be the matrix of steady-state gains of the transfer function matrix $\mathbf{G}(s)$ as s turns to zero. The steady-state form of the model becomes

$$\mathbf{G}(0) = \begin{bmatrix} G_{11}(0) & G_{12}(0) \\ G_{21}(0) & G_{22}(0) \end{bmatrix} = \begin{bmatrix} K_{11} & K_{12} \\ K_{21} & K_{22} \end{bmatrix} \quad (2)$$

The derivation of RGA through fundamental principles, as well as the matrix approach for RGA multiplication, has been explained in [31]. As a result, the methodology for determining RGA in a 2×2 system is articulated as

$$\Lambda = \begin{bmatrix} \lambda_{11} & \lambda_{12} \\ \lambda_{21} & \lambda_{22} \end{bmatrix} = \mathbf{K}(\mathbf{K}^{-1})^T \quad (3)$$

The RGA of the steady-state gain matrix $\mathbf{G}(0)$ is defined in [27, 30, 31], where $(\mathbf{K}^{-1})^T$ is the transposition of (\mathbf{K}^{-1}) . The corresponding relative gains can be calculated as

$$\Lambda = \begin{bmatrix} \lambda_{11} & \lambda_{12} \\ \lambda_{21} & \lambda_{22} \end{bmatrix} = \begin{bmatrix} \lambda_{11} & 1 - \lambda_{11} \\ 1 - \lambda_{11} & \lambda_{11} \end{bmatrix} \quad (4)$$

From the definition of the inverse of a matrix, the following steps are followed to find the RGA gain:

$$\mathbf{K}^{-1} = \frac{1}{|\mathbf{K}|} \begin{bmatrix} K_{22} & K_{12} \\ K_{21} & K_{11} \end{bmatrix} \quad (5)$$

where $|\mathbf{K}|$, the determinant of \mathbf{K} is given by

$$|\mathbf{K}| = K_{11}K_{22} - K_{12}K_{21} \quad (6)$$

and taking the transpose of the matrix given in (5), we obtain

$$(\mathbf{K}^{-1})^T = \frac{1}{|\mathbf{K}|} \begin{bmatrix} K_{22} & -K_{21} \\ -K_{12} & K_{11} \end{bmatrix} \quad (7)$$

Now carry out a term-by-term multiplication of the elements of the matrices in (5) and (7), and the following is obtained.

$$\lambda_{11} = \lambda_{22} = \frac{1}{1 - \frac{K_{12}K_{21}}{K_{11}K_{22}}} = \frac{K_{11}K_{22}}{K_{11}K_{22} - K_{12}K_{21}} \quad (8)$$

while the $\lambda_{12} = \lambda_{21} = 1 - \lambda_{11}$

With regards to the steady-state gains presented in (2), the RGA matrix is obtained as given as

$$\Lambda(\mathbf{K}) = \begin{bmatrix} 0.9817 & 0.0183 \\ 0.0183 & 0.9817 \end{bmatrix} \quad (9)$$

To interpret the resulting RGA matrix of (9), the recommendations as presented in [31] are followed. The recommended pairing's steady-state input-output relationship is thus as follows:

$$\begin{bmatrix} h(0) \\ \varepsilon_{gcz}(0) \end{bmatrix} = \begin{bmatrix} G_{11}(0) & G_{12}(0) \\ G_{21}(0) & G_{22}(0) \end{bmatrix} = \begin{bmatrix} -2.980 & 0.135 \\ 0.004 & 0.0097 \end{bmatrix} \quad (10)$$

The pairing rule known as RGA does not consider the stability of the resulting control structure. For that reason, the resultant control operational stability must be checked. This is done according to the rule of the Niederlinski index as presented by [28, 32]

A. Internal Model Controller Design

When dealing with the control of interconnected systems, three primary challenges arise. The first challenge revolves around the practical constraints concerning the quantity and arrangement of feedback loops, which favor the implementation of decentralized control structures. The presence of hesitations in both subsystems and interconnections adds additional concern. The third challenge involves ensuring the dependability of control systems in cases of component failures. This holds particular significance within interconnected systems, where malfunctions can manifest as complete shutdowns or partial deterioration in each subsystem. These aspects are among the analyses considered in the discussion concerning the utilization of both RGA and IMC techniques for this paper.

Eq. (11) presents an equivalent predictable control to the internal model controller, with the relationships between the conventional feedback controller, $G_C(s)$, and the internal model controller, $C(s)$. Equation (11) is useful in the controller design discussion and can be easily followed.

$$G_C(s) = \frac{C(s)}{1 - G(s)C(s)} \quad (11)$$

Once the controller design is accomplished, the implementation of Fig. 2 is carried out within Simulink as a representation of a multi-variable system.

When putting the IMC scheme into practice, there are practical considerations that must be accounted for, as outlined in [24, 31]. Consequently, the IMC design procedure has been adjusted through a sequence of stages, including process model factorization, controller specification, and filter design, as specified by (12) and (13) provided below:

$$C(s) = \frac{1}{G(s)} f(s) \quad (12)$$

$$f(s) = \frac{1}{(\lambda s + 1)^n} \quad (13)$$

where $f(s)$ is a filter, λ is a flexible variable filter factor and n is a factor that can be used to ensure proper control. The IMC controller, $C(s)$, is converted to the

conventional form, $G_C(s)$, for implementation. This is accomplished by using (11).

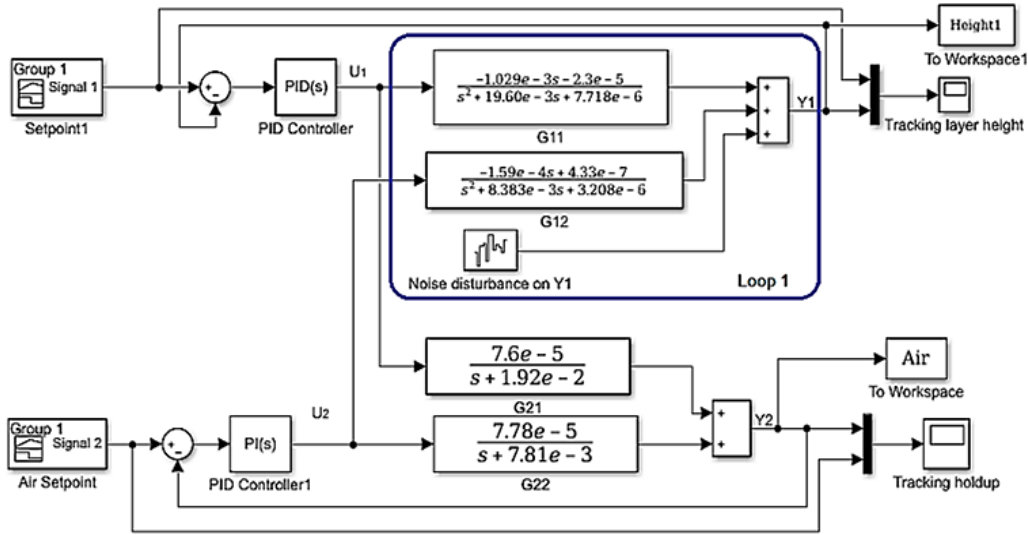


Fig. 2. Simulink block diagram representation of the decentralized coupled system model.

The details of the IMC design procedure have been reviewed and will now be adhered to in order to formulate the control parameters for both the froth layer height and air holdup.

B. Design Internal Model Control-Based PID Control for the Froth Layer Height

The IMC design methodology, along with the discussed practical considerations, was applied to design a controller for the froth part of the system, characterized by the following transfer function:

$$G_{11}(s) = \frac{-1.029 \times 10^{-3} s - 2.3 \times 10^{-5}}{s^2 + 19.60 \times 10^{-3} s + 7.718 \times 10^{-6}} \quad (14)$$

$$= \frac{-3(44.4s + 1)}{129.6 \times 10^3 s^2 + 2.5 \times 10^3 s + 1}$$

The process model is subjected to factorization using the proposed IMC design approach. By separating the process into parts, its model is divided into segments that are either invertible or non-invertible, based on the factorization steps presented in subsection A, therefore,

$$G_{11}(s) = G_{11+}(s)G_{11-}(s)$$

$G_{11+}(s)$ contains all the non-invertible aspects with a steady-state gain. $G_{11-}(s)$ is the remaining invertible part of (14), $G_{11+}(s) = 44.4s + 1$, and

$$G_{11-}(s) = \frac{-3}{129.6 \times 10^3 s^2 + 2.5 \times 10^3 s + 1}$$

Therefore, from the IMC controller design specifications and filter design, the closed-loop response is generally given by

$$C(s) = \frac{1}{G_P(s)} f(s) \quad (15)$$

Thus, the IMC method as specifically described is used for the closed-loop control design of the front layer height with a filter element included as presented (16) and described by [31]

$$C_{11}(s) = G_{11-}(s)^{-1} f(s) = \frac{P(s)}{-3(\lambda s + 1)} \quad (16)$$

where $P(s) = 130 \times 10^3 s^2 + 2.5 \times 10^3 s + 1$.

Rewriting the equivalent predictable control presented in (11), calculating the controller parameters for the froth layer loop, and using the process model formed in (14) and the filtered control element presented in (16), we obtain

$$G_{C_{11}}(s) = \frac{C_{11}(s)}{1 - G_{11}(s)C_{11}(s)}$$

$$= \frac{\frac{P(s)}{-3(\lambda s + 1)}}{1 - \left(\frac{-3(44.4s + 1)}{P(s)} \times \frac{P(s)}{-3(\lambda s + 1)} \right)} \quad (17)$$

Solving and simplifying (17) will result in the controller, expressed as

$$G_{C_{11}}(s) = \frac{P(s)}{-3\lambda s - 3 + 133s + 3}$$

$$= \frac{130 \times 10^3 s^2 + 2.5 \times 10^3 s + 1}{130\lambda s} + \frac{2.5 \times 10^3 s}{130\lambda s} + \frac{1}{130\lambda s} \quad (18)$$

$$= \frac{2.5 \times 10^3}{130\lambda} \left(1 + \frac{1}{2.5 \times 10^3 s} + 52s \right)$$

Now the structure is of an ideal PID structure, therefore, the PID control parameters of the froth layer height led to the following:

$$K_p = \frac{2.5 \times 10^3}{130\lambda}$$

$$\tau_I = \frac{1}{2.5 \times 10^3} \tau_D = 52$$

To ensure proper control and through severally tests λ is selected to be -0.27 .

C. IMC-Based PID Feedback Control Design for the Air Holdup Control Loop

The controller for the air hold-up is designed following the procedure for IMC controller design and practical issues that need to be considered. Design a controller for the air holdup system whose transfer function is given by

$$G_{22}(s) = \frac{7.78 \times 10^{-5}}{s + 7.981 \times 10^{-3}} = \frac{9.75 \times 10^{-3}}{125.3s + 1} \quad (19)$$

Using IMC strategies and converting it to a conventional feedback form, we obtain

$$G_{22-}(s)^{-1} = \frac{125.3s + 1}{9.75 \times 10^{-3}} \quad (20)$$

Therefore, the IMC specifications and filter design are produced as

$$C_{22}(s) = \frac{1}{G_{22-}(s)} f(s) = \frac{125.3s + 1}{9.75 \times 10^{-3}(\lambda s + 1)} \quad (21)$$

Now design the controller parameters for the air holdup closed-loop response using an IMC-based PID feedback structure. Combining (19) and (21), the equivalent predictable control based on the air holdup loop becomes

$$G_{C_{22}}(s) = \frac{C_{22}(s)}{1 - G_{22}(s)C_{22}(s)} = \frac{\frac{125.3s + 1}{9.75 \times 10^{-3}(\lambda s + 1)}}{1 - \left(\frac{9.75 \times 10^{-3}}{125.3s + 1} \times \frac{125.3s + 1}{9.75 \times 10^{-3}(\lambda s + 1)} \right)} \quad (22)$$

Therefore, the PID controller for the air holdup loop generates a PI controller presented in (23) because of the order of the system:

$$G_{C_{22}}(s) = \frac{125.3}{9.75 \times 10^{-3} \lambda} \left(1 + \frac{1}{125.3s} \right) \quad (23)$$

The resulting PI control parameters are:

$$K_P = \frac{125.3}{9.75 \times 10^{-3} \lambda}, \quad \tau_I = \frac{1}{125.3}$$

To ensure proper control Lambda (λ) is selected to be 1.6. Therefore, the IMC design based on the PID feedback control design has been concluded and resulted in control parameters presented in Table I.

TABLE I: DESIGNED PID CONTROL PARAMETERS DESIGNED BASED ON IMC

Parameters	Froth layer height	Air holdup
Proportional	-71	8032
Integral	0.0004	0.008
Derivative	52	0
Tuned filter factor Lambda & n	-0.27	1.6

Since all the necessary control parameters have been successfully obtained, the following section presents the simulation results.

III. MODEL EVALUATION AND RESULTS

Matlab/Simulink is used for the closed-loop simulation of the coupled flotation system. The simulated cases are presented below.

Case study 1: For this particular instance, the setpoint for the froth layer height is initiated at 40 cm and gradually raised to 60 cm. Concurrently, the holdup begins at 10% and is elevated to 18% by the 10th second. The simulated outcomes for this scenario are illustrated in Fig. 3 and Fig. 4.

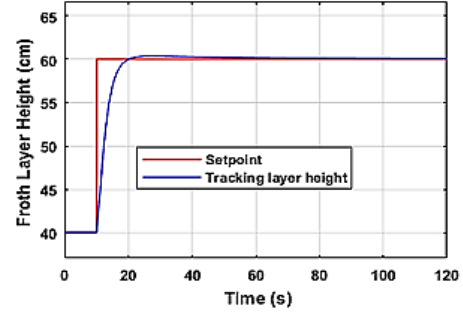


Fig. 3. Case 1: Closed-loop response of the froth layer height zone.

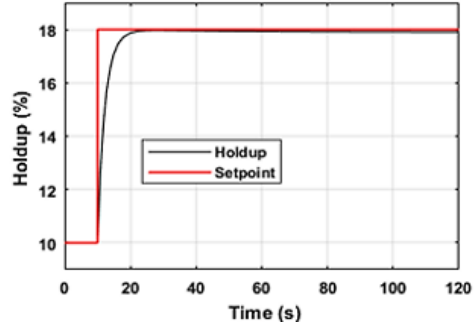


Fig. 4. Case 1: Closed-loop response of the air holdup zone.

Case study 2: In this scenario, the initial setpoint for the froth layer height is established at 50 cm. At the 10th second, a setpoint change is implemented, shifting the signal from 50 cm to 70 cm and then reducing it to 60 cm by the 60th second. Meanwhile, the holdup remains steady at an initial value of 10% and is raised to 18% by the 10th second. This real-world application involves the accumulation of a substantial quantity of mineral particles from the collection zone, leading to an increase in the froth layer. Then, the decrease in froth layer height at the 60-second mark is achieved by introducing wash water at the column's top, serving to eliminate any remaining undesirable minerals. The executed results for this case are presented in Fig. 5 and Fig. 6.

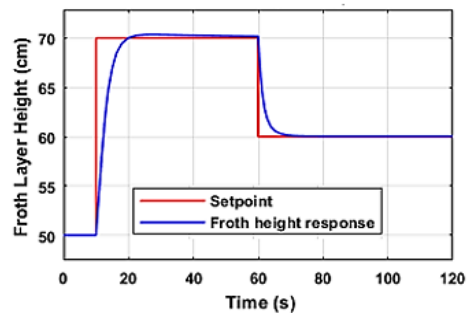


Fig. 5. Case 2: Closed-loop response of the froth layer height.

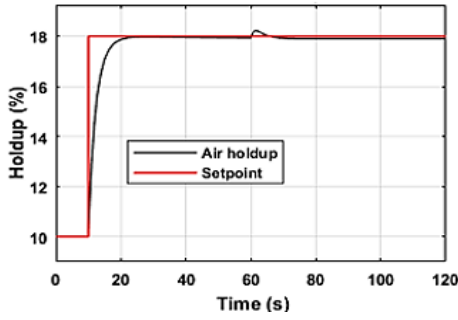


Fig. 6. Case 2: Closed-loop response of the air holdup zone.

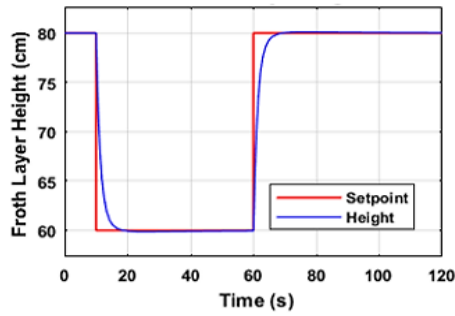


Fig. 7. Case 3: Closed-loop response of the froth layer height.

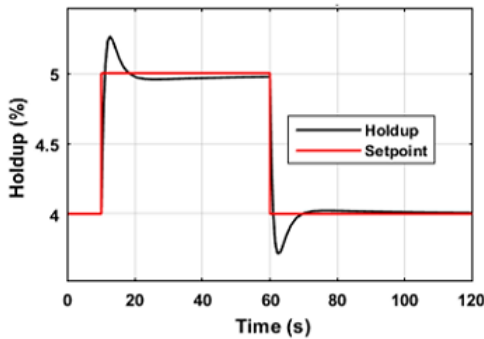


Fig. 8. Case 3: Closed-loop response of the air holdup zone.

Case study 3: In this scenario, both the setpoints for the froth layer height and Air holdup are altered by adjusting their setpoints to observe the operational behavior of the system. The froth layer height in Fig. 7 is initially set at 80 cm, while the applied holdup is set to 4%. Irregular changes are introduced at the 10 s mark, wherein the setpoint for the layer height is reduced to 60 cm. Adding wash water on top of the column results in a subsequent drop in the froth layer height. Fig. 8 illustrates a setpoint change for the holdup, starting from 4% and increasing to 5% at 10 s, followed by a decrease from 5% back to 4%. This is undertaken to assess the closed-loop system’s ability to track irregular setpoint changes and discover if the system can effectively respond to such changes within a short response time.

Table II represents the characteristic response of the flotation system focusing on rise time, settling time, and overshoot. Analysis of these characteristics reveals that the duration required for the system to reach its maximum value was reduced in Case 3 compared to the first two cases. However, the extent to which the value exceeded

the desired level was greater than what was seen in the earlier cases.

TABLE II: TRANSITION PROCESSES PERFORMANCE INDEXES

Cases	Loop zone	Rise time	Settling time	Overshoot
Case 1	Height	5.48	18.7	0.036
	holdup	4.86	18.3	0.03
Case 2	Height	1.80	67.5	0.036
	holdup	4.84	64.5	0.05
Case 3	Height	0.49	66.0	0.01
	holdup	0.004	68.5	0.26

By utilizing a time-correlated random sequence, the system encounters a disruption in its output by introducing a noise disturbance, at the output point as illustrated in Fig. 2. This procedure was conducted to examine the impacts of the disturbance on the froth layer height and air holdup area, with each loop individually exposed to the disturbance. The outcomes of this investigation are presented in Fig. 9 and Fig.10.

When shifting the disturbance from loop 1 to loop 2 while keeping the noise magnitudes constant, both the froth layer height and holdup loops encounter overshoots of 1.452 and 1.25, respectively. Because of limitations in available space, the outcomes of these evaluations are exclusively displayed in Case 4. Nevertheless, comprehensive analyses have consistently verified that as the magnitude of the disturbance increases, the system encounters higher degrees of fluctuations.

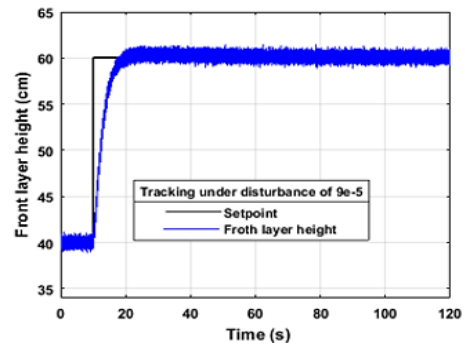


Fig. 9. Case 4: Closed-loop response of the froth layer height.

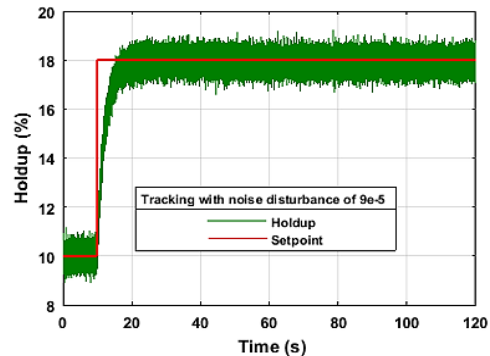


Fig. 10. Case 4: Closed-loop response of the air holdup zone.

IV. DISCUSSION

This paper introduces an improved method for the design of decentralized PID controllers aimed at controlling different parameters within column flotation.

The approach employs the Relative Gain Array (RGA) technique. The assessment of setpoint tracking has been successfully conducted. The findings from the investigation demonstrate that both the trajectory behaviors of the froth layer height and air holdup indeed align with the variations in setpoints. The conducted investigation has proven to be successful in terms of setpoint tracking and good settling time. The designed controller based on decentralization of the PID controllers using IMC and RGA techniques has proven to be an effective control strategy for set-point variations and disturbance influence. Decomposing the process model into decentralized components has shown to be a successful approach in mitigating the impact of system interactions in closed-loop control, ensuring stable system behavior. The results presented affirm the potential for model transformation using both Matlab/Simulink and TwinCAT software environments.

V. CONCLUSION

The PID controllers designed through the implementation of IMC and RGA techniques for the flotation systems have operated following the specified requirements. All the results shown demonstrated successful performance in terms of set-point tracking and disturbance rejection. Nevertheless, it is also noted that the designed PID controllers could not successfully embrace the overshoot of the air hold-up loop for this coupled multi-variable flotation plant process. This limitation is shown in Case 3, where the froth height or holdup control valves are not softly adjustable. Furthermore, an evaluation based on the performance of the control parameters developed for the decentralized coupled system was carried out, by varying levels of random noise introduced into both the froth layer height loop and the holdup loop. Observations reveal that the system exhibits overshooting when encountering substantial variations in set points and disturbances. This emphasizes the importance of sustained advancement in the development of new or enhanced methodologies that seek alternative ways to overcome such challenges. An evaluation of the controller parameters developed for the decentralized coupled system's performance is carried out by varying levels of random noise introduced into both the froth layer height loop and the holdup loop. When designing control parameters for flotation or any MIMO systems, it is important to use a control technique that can handle any range of system changes and consider decoupling the system to minimize its interactions. Therefore, future research, for now, will look at the use of Programmable Logic Controllers (PLC) for real-time implementation of the considered technique, and the design of an improved controller to eliminate the minor overshoot due to heavy variations similar to Case 3 and Case 4.

CONFLICT OF INTEREST

The authors declare no conflict of interest.

AUTHOR CONTRIBUTIONS

N. Tshemese-Mvandaba, conducted the research, wrote the paper, and analyzed the data; M. Mnguni, reviewed, and edited the paper; all authors approved the final version.

ACKNOWLEDGMENT

This work was supported by the THRIP/NRF project, "Centre for Real-Time Distributed Systems (CRTDS),"

REFERENCES

- [1] T. A. M. Euzebio, M. T. D. Silva, and A. S. Yamashita, "Decentralized PID controller tuning based on nonlinear optimization to minimize the disturbance effects in coupled loops," *IEEE Access*, vol. 9, pp. 156857–156867, 2021.
- [2] S. S. Anchan and C. S. Rao, "Robust decentralized proportional–integral controller design for an activated sludge process," *Asia-Pacific Journal of Chemical Engineering*, 2020. DOI: 10.1002/apj.2531
- [3] J. Sivadasan, M. W. Iruthayarajan, A. A. Stonier, and A. Raymon, "Design of cross-coupled nonlinear PID controller using single-objective evolutionary algorithms," *Hindawi Mathematical Problems in Engineering*, vol. 2023, #7820047, 2023.
- [4] Hany, A. K. Said, E. Mohamed, and I.M. Mohamed, "Adaptive neuro-fuzzy self-tuned-PID controller for stabilization of core power in a pressurized water reactor," *International Journal of Robotics and Control Systems*, vol. 3, no. 1, pp. 1–18, 2023.
- [5] P. Quintanilla, S. J. Neethling, and P. R. Brito-Parada, "Modelling for froth flotation control: A review," *Minerals Engineering*, vol. 162, #106718, Nov. 2021.
- [6] V. T. Vu, Q. H. Tran, T. L. Pham, and P. N. Dao, "Online actor-critic reinforcement learning control for uncertain surface vessel systems with external disturbances," *International Journal of Control, Automation and Systems*, vol. 20, no. 3, pp. 1029–1040, 2022.
- [7] X. Zhou, Q. Wang, R. Zhang, and C. Yang, "A hybrid feature selection method for production condition recognition in froth flotation with noisy labels," *Minerals Engineering*, vol. 153, #106201, 2020.
- [8] V. S. Bhat, I. Thirunavukkarasu, and S. S. Priya, "Design and implementation of decentralized PI controller for pilot plant binary distillation column," *International Journal of ChemTech Research*, vol. 10, no.1, pp. 284–294, 2017.
- [9] V. D. Hajare, B. M. Patre, A. A. Khandekar, and G.M Malwatkar, "Decentralized PID controller design for TITO processes with experimental validation," *International Journal of Dynamics and Control*, vol. 5, no. 3, pp. 583–595, 2017.
- [10] T. Yahui, A. Maryam, L. Xiaoli, L. Fei, and D. Stevan, "Three-phases dynamic modelling of column flotation process," *IFAC-Papers On-Line*, vol. 51, no. 21, pp. 99–104, 2018.
- [11] X. Luan, Q. Chen, and F. Liu, "Centralized PI control for high dimensional multivariable systems based on equivalent transfer function," *ISA Trans.*, vol. 53, no. 4, pp. 1554–1561, 2014.
- [12] M. Ai, Y. Xie, Z. Tang, J. Zhang and W. Gui, "Deep learning feature-based setpoint generation and optimal control for flotation processes," *Information Sciences*, vol. 578, pp. 644–658, 2021. <https://doi.org/10.1016/j.ins.2021.07.060>, 2021
- [13] M. A. Persechini, F. Jota, and A. E. Peres, "Dynamic model of a floatation column," *Minerals Engineering*, vol. 13, no. 14–15, pp. 1465–1481, 2000.
- [14] M. A. M. Persechini, A. E. C. Peres, and F. G. Jota, "Control strategy for a column flotation process," *Control Engineering Practice*, vol. 12, no. 8, pp. 963–976, 2004.
- [15] J. M. C. Vale and G. F. Azevedo, "Predictive control applied to a mathematical model of a floatation column," *International Journal of Advanced Engineering Research and Science*, vol. 5, no. 10, pp. 110–114, 2018.
- [16] L. Zhang and D. Xu, "Flotation bubble size distribution detection based on semantic segmentation," *IFAC PapersOnLine*, vol. 53,

no. 2, pp. 11842–1184, 2020.

- [17] N. Tshemese-Mvandaba and M. E. S. Mnguni, “Decentralized proportional-integral controller based on dynamic decoupling technique using Beckhoff TwinCAT-3.1,” *International Journal of Electrical and Computer Engineering*, vol. 13, no. 3, pp. 2721–2733, 2023.
- [18] J. D. le Roux, D. J. Oosthuizen, S. Mantsho, and I. K. Craig, “A survey on the status of industrial flotation control,” *IFAC PapersOnLine*, vol. 53, no. 2, pp. 11854–11859, 2020.
- [19] L. G. Bergh and J. B. Yianatos, “Flotation column automation: State of the art,” *Control Engineering Practice*, vol. 11, no. 1, pp. 67–72, 2003
- [20] B. J. Shean and J. J. Cilliers, “A review of froth flotation control,” *International Journal of Mineral Processing*, vol. 100, no. 3–4, pp. 57–71, 2011.
- [21] M. Derhy, Y. Taha, R. Hakkou, and M. Benzaazoua, “Review of the main factors affecting the flotation of phosphate ores,” *Minerals*, 2020. doi:10.3390/min10121109
- [22] D. Hernandez-Alcantara, L. Amezquita-Brooks, and R. Morales-Menendez, “Decentralized controllers for the steering and velocity in vehicles,” *IFAC-PapersOnLine*, vol. 50, no. 1, pp. 3708–3713, 2017.
- [23] N. Tshemese-Mvandaba, R. Tzoneva, and M. E. S. Mnguni, “Decentralised PI controller design based on dynamic interaction decoupling in the closed-loop behaviour of a flotation process,” *International Journal of Electrical and Computer Engineering*, vol. 11, no. 6, pp. 4865–4880, 2021.
- [24] V. Eduardo, R. B. Lorenzo, R. M. Roman, F. G. Carlos, C. V. Fernando, and V. G. Hector “Modeling and energy-based model predictive control of high-pressure grinding roll,” *Minerals Engineering*, vol. 134, pp. 7–15, April 2019.
- [25] G. Pujol, J. Rodellar, J. Rossell, and F. Pozo, “Decentralised reliable guaranteed cost of uncertain systems: An LMI design,” *IFAC PapersOnline*, vol. 16, pp. 263–268, 2007. <https://doi.org/10.1049/iet-cta>
- [26] D. Chen and D. E. Seborg, “Relative gain array analysis for uncertain process models,” *AIChE. Journal*, vol. 48, no. 2, pp. 302–310, 2002.
- [27] E. H. Bristol, “On a new measure of interaction for multivariable process control,” *IEEE Trans. on Automatic Control*, vol. 11, no. 1, pp. 133–134, 1966.
- [28] S. P. Bandsode and C. S. Besta “Centralized and decentralized control system for reactive distillation diphenyl carbonate process,” in *Distillation Processes - From Solar and Membrane Distillation to Reactive Distillation*, V. Steffen Ed. 2022.
- [29] M. T. Munir, W. Yu, and B. R. Young, “Recycle effect on the relative exergy array,” *Chemical Engineering Research and Design*, vol. 90, no. 1, pp. 110–118, 2012.
- [30] T. O. Ajayi and I. S. Ogbob, “Determination of control pairing for higher order multivariable systems by the use of multi-ratios,” vol. 3, no. 3, pp. 1–5, 2012.
- [31] B. Ogunnaike and H. Ray, *Process Dynamics, Modeling, and Control*, 1994.
- [32] A. Jain and B. V. Babu, “Sensitivity of relative gain array for processes with uncertain gains and residence times,” *IFAC PapersOnLine*, vol. 49, no. 1, pp. 486–491, 2016.

Copyright © 2024 by the authors. This is an open access article distributed under the Creative Commons Attribution License (CC BY-NC-ND 4.0), which permits use, distribution and reproduction in any medium, provided that the article is properly cited, the use is non-commercial, and no modifications or adaptations are made.



Nomzamo Tshemese-Mvandaba is a full-time Electronics and Process Control Lecturer, She’s also an Extended Curriculum Programme Coordinator in the Department of Electrical, Electronics and Computer Engineering (DEECE) at Cape Peninsula University of Technology (CPUT), Cape Town. She received a B.Tech. degree in electrical engineering from the Cape Peninsula University of Technology in 2011, her Master of Technology degree from the Cape Peninsula University of Technology in 2015, and her doctoral degree at CPUT in 2022. Her research interest is in linear and non-linear multivariable system modeling, modern controller design techniques, process control instrumentation, automation, and PLC applications.



Mkhululi Elvis Siyanda Mnguni received a B-tech degree in Electrical Engineering from the Cape Peninsula University of Technology in 2006 and his Master degree from the Cape Peninsula University of Technology in 2014. Currently, employed as a Research Scholar and Lecturer. He completed his Doctor of Engineering. degree at the Cape Peninsula University of Technology in 2018. His research interests are Power system stability, protection, substation automation, process instrumentation, and PLC applications. He can be contacted at mngunim@cput.ac.za